

Refereed Proceedings

The 13th International Conference on

Fluidization - New Paradigm in Fluidization

Engineering

Engineering Conferences International

Year 2010

HEAT TRANSFER TO IMMERSED
COOLING TUBES AND PARTICLES
IN A FLUIDIZED BED REACTOR

Y. Kobayashi, Y. Mori* A. Goto†

H.T. Bi J.R. Grace‡

*Sumitomo Chemical Company

†Sumitomo Chemical Company, gotoa2@sc.sumitomo-chem.co.jp

‡University of British Columbia

This paper is posted at ECI Digital Archives.

http://dc.engconfintl.org/fluidization_xiii/81

HEAT TRANSFER TO IMMERSSED COOLING TUBES AND PARTICLES IN A FLUIDIZED BED REACTOR

Y. Kobayashi, Y. Mori, A. Goto,
Sumitomo Chemical Company, Japan,

H.T. Bi and J.R. Grace
University of British Columbia, Vancouver, Canada

Abstract: A simple heat transfer model is utilized to determine the heat transfer coefficients for multiple tubes immersed in an industrial fluidized bed reactor supporting an exothermic reaction. From the temperatures at their outlets, superheating occurs in some blocks of tubes, but not in others. A four-zone heat transfer model is then used to evaluate the axial and lateral temperature differences due to the existence of a bottom un-cooled entrance zone and two cooled zones, corresponding to the regions where superheating does and does not occur.

1. INTRODUCTION

In many fluidized beds where exothermic reactions are carried out, cooling surfaces are immersed in the bed in the form of coils or hairpin tubes to maintain desired temperatures (1, 2, 3). Water is the most common cooling fluid. As it travels through the tubes, the water temperature increases from its feed temperature to the boiling point, and often well beyond as superheating occurs. Although fluidized beds are known for their temperature uniformity, there is also a possibility of temperature gradients between cooler and hotter regions of the bed. Being able to regulate the temperature inside the tubes to maintain consistent product quality and overall safety is essential. Therefore it is crucial to understand the coupling between the heat transfer on the outside and inside of the cooling coils.

In an exothermic fluidized bed reactor operated by Sumitomo Chemical Company, the exit temperature of coolant from different banks of heat transfer tubes indicated that superheating of steam was occurring in some tubes, but not others. In the latter case, the exit temperature was essentially equal to the boiling point of water at the pressure inside the tubes, so that partial boiling was occurring. This paper considers a simple mechanistic model based on the premise that each of the two types of tubes (those where complete boiling plus superheating occurs, and

those where incomplete boiling occurs) can be treated as zones in series. This allows calculation of the proportion of the total surface area occupied by heating of sub-cooled liquid, boiling, and superheating zones. A separate but related model is then utilized to predict the difference in bed temperature between zones in which the two classes of tubes are found, and in the un-cooled regions underneath them.

2. COOLING TUBE BOILING/SUPERHEATING MODEL

The calculations are based on an industrial fluidized bed reactor with 12 blocks of hairpin tubes with water flow regulated by control valves. There are 152 tubes of o.d. 89.1 mm and i.d. 78.1 mm in total, with variable numbers, and hence variable heat transfer area, in each block. The configuration is shown in Figs. 1 and 2. Water comes from a common header, entering at 200°C and 3.0 MPag. The bed temperature is 400°C, the overall water flow 1.14 kg/s and overall steam production 0.36 kg/s. Temperatures for each block, measured only at the outlet indicated that superheating was occurring in some blocks, while partial boiling was taking place in the others. Close examination of the data revealed that the blocks could be divided into two groups:

Group A: The water in these blocks clearly boils completely, and the resulting steam is then superheated from the boiling temperature of 236°C to ~340°C. We call these tubes “**Superheated steam producers**” and denote them by subscript ‘SP’. Their total length, including horizontal sections between hairpins, is 48.54 m.

Group B: The water in these blocks only partially boiled, with the outlet temperature being close to the boiling temperature. We call these tubes “**Non-complete boilers**” and denote them by ‘NB’. The total length of these tubes is 79.11 m.

Each of these two groups is treated as an overall entity, with minor differences among the blocks within each of the groups ignored. The total length of the SP tubes is divided into 3 portions:

L_1 = length to heat liquid water from entry temperature of 200°C to boiling point;

L_2 = length to boil all of the water in the SP group at the boiling point;

L_3 = length to superheat the steam from 236°C to the exit temperature of 340°C.

Clearly $L_1 + L_2 + L_3 = 48.54$ m. The overall heat transfer coefficient in the sections where water is being heated or boiling is occurring is assumed to be constant with the major resistance on the fluidized bed side. On the other hand, in the portion where steam is being superheated, the major resistance is on the steam side (inside), with heat transfer coefficient designated by h_{steam} . Let m_{SP} be the water flow rate to the SP tubes. We then do a heat balance on each of the three portions of this tube:

L_1 : Heat gained by water in this interval = heat transferred to this portion of tube.

L_2 : Heat required to vaporize the water = heat transferred to this portion

L_3 : Heat to superheat the steam = heat transferred to third portion of tubes. Similarly, the length of the NB tubes is divided into two portions, L_1^* , where liquid water is heated to the boiling temperature, and L_2^* , where partial boiling occurs. Heat balances are again performed on both portions as above. In addition, $L_1^* + L_2^* = 79.11$ m and $m_{NB} + m_{SP} = 1.14$ kg/s (water balance). Also $f \times m_{NB} + m_{SP} = 0.36$ kg/s (steam balance), where f is the fraction of the NB stream converted to steam. To calculate the heat transfer coefficient on the steam side, h_{steam} , in the portion of the SP tubes where superheating occurs, we use the well-known Dittus-Boelter equation, with steam properties evaluated at an average temperature and pressure.

3. PREDICTIONS FROM TRANSFER MODEL

The 10 equations with 10 unknowns were solved by Polymath software leading to $L_1 = 1.06$ m; $L_2 = 14.07$ m; $L_3 = 33.41$ m; $L_1^* = 17.37$ m; $L_2^* = 61.74$ m, $m_{SP} = 0.0660$ kg/s; $m_{NB} = 1.0785$ kg/s; $f = 0.2685$; $h = 182.2$ W/m²K; $h_{steam} = 22.3$ W/m²K. A schematic showing the system analyzed is shown in Fig.3. This heat transfer coefficient is less than the outside (bed-to-surface) heat transfer coefficient expected for group A particles. One reason for this is that it is an overall heat transfer coefficient, so that conduction resistance through the tube walls, resistance on the water/steam side, and fouling resistance (if appreciable) will lower the value to some extent. However, the main reason is that the tubes are not fully immersed in the bed. Heat transfer decreases with height in the freeboard. While there are no accurate methods of predicting this decrease, the empirical equation of George and Grace (4), although based on horizontal tubes in the freeboard, gives a good prediction when coupled with the TDH estimated from the well-known graphical correlation of Zenz and integrated numerically over the height.

4. FOUR-ZONE BED-SIDE HEAT TRANSFER MODEL

The heat transfer tubes begin well above the distributor to avoid erosion, creating an un-cooled zone near the distributor. It is shown above that the heat transfer tubes operate under different conditions, with only some producing superheated steam. If heat is released uniformly across the reactor cross-section, heat removal will differ in regions where tubes are subject to superheating from regions where there is only boiling. As a result, there will be a temperature difference between the regions. Given the vertical and horizontal partitioning, the reactor is divided into four zones as illustrated in Fig 4. A four-zone heat transfer analysis is then carried out to estimate the temperature differences among the four regions in the reactor. In each zone, heat is generated from the reaction, exchanged with neighbouring zones by gas and particle convection, and removed by heat transfer

tubes. From energy balances for each zone, one can derive four equations:

$$\text{Zone E1: } \Delta H_r \phi_{E1} = \rho_g US_1 C_{pg} (T_{E1} - T_0) + \eta W_{a1} C_{pp} (T_{E1} - T_{B1}) + W_{rE} C_{pp} (T_{E1} - T_{E2})$$

$$\text{Zone E2: } \Delta H_r \phi_{E2} = \rho_g US_2 C_{pg} (T_{E2} - T_0) + \eta W_{a2} C_{pp} (T_{E2} - T_{B2}) + W_{rE} C_{pp} (T_{E2} - T_{E1})$$

$$\text{Zone B1: } \Delta H_r \phi_{B1} = \rho_g US_1 C_{pg} (T_{B1} - T_{E1}) + \eta W_{a1} C_{pp} (T_{B1} - T_{E1}) + W_{rB} C_{pp} (T_{B1} - T_{B2}) + h_1 A_1 (T_{B1} - T_{w1})$$

$$\text{Zone B2: } \Delta H_r \phi_{B2} = \rho_g US_2 C_{pg} (T_{B2} - T_{E2}) + \eta W_{a2} C_{pp} (T_{B2} - T_{E2}) + W_{rB} C_{pp} (T_{B2} - T_{B1}) + h_2 A_2 (T_{B2} - T_{w2})$$

where the left sides represent heat released by reaction, the first terms on the right account for vertical gas convection, the second for axial solids convection and the third for radial solids convection. ϕ is the conversion of reactant in each zone, S the cross-sectional area, A the surface area of cooling tubes (assumed to be proportional to the cross-sectional area), W_a the axial solids mixing rate, W_r the radial solids mixing rate, h the average heat transfer coefficient between the bed and cooling tubes, and T_w the water/steam temperature inside the cooling tubes.

The solids circulation rate in free bubbling beds without internals can be related to the bubble flow (Z) by:

$$W_{a1} = (f_w + f_d)(1 - \varepsilon_{mf}) \rho_p G_{B1} \quad \text{and} \quad W_{a2} = (f_w + f_d)(1 - \varepsilon_{mf}) \rho_p G_{B2} \quad (1)$$

$$G_{B1} = 0.8(U - U_{mf}) S_1 \quad \text{and} \quad G_{B2} = 0.8(U - U_{mf}) S_2 \quad (2)$$

$$\text{with } S_1 = S \times A_1 / (A_1 + A_2) \quad \text{and} \quad S_2 = S \times A_2 / (A_1 + A_2) \quad (3)$$

where f_w is the wake fraction of bubbles, f_d the fraction of solids carried by the drift produced by bubble motion, and G_s the bubble gas flow rate. For fine Group A particles used in most gas-phase catalytic reactors, conservative estimates of the various parameters are: $f_w = 0.37$ (6), $f_d = 0.36$ (10) and $\varepsilon_{mf} = 0.56$. Due to the heat transfer tubes in the heat exchange zone, the solids circulation will be retarded somewhat. A correction coefficient, η , is thus introduced into equation (1). We have assigned a value of 0.8 to η given the degree of blockage in the current case.

Horizontal mixing in bubbling fluidized beds is generally an order lower than axial mixing. Hence, the lateral solids flux is taken to be 10% of the axial flux:

$$W_{rE} = 0.1 \frac{W_{a1} + W_{a2}}{S} (kD H_E) \quad \text{and} \quad W_{rB} = 0.1 \frac{W_{a1} + W_{a2}}{S} [kD(H - H_E)] \quad (9)$$

where kD represents the perimeter of the interface between the two horizontal zones, D is the reactor diameter, and H_E and H represent the height of the bottom un-cooled region and the expanded bed height, respectively. The interface area between the two zones is determined based on the superheated steam heat exchange length and

the surrounding area, with $k = 2.7$ in the current analysis.

The heat release rate from the reaction in each zone is estimated from a two-phase fluidized bed reactor model (8), incorporating a grid zone defined by the vertical jet penetration length, L_j , estimated from the Merry (9) correlation. The interphase mass transfer rate, K_j , between the jet and dense phase, is approximated as 0.1 m/s in the current analysis.

$$\Delta H_r \phi_{E1} = Q_{rx} \left(\frac{S_1}{S} \right) X_{H_E} \quad \text{and} \quad \Delta H_r \phi_{E2} = Q_{rx} \left(\frac{S_2}{S} \right) X_{H_E} \quad (4)$$

$$\Delta H_r \phi_{E1} = Q_{rx} \left(\frac{S_1}{S} \right) (X_H - X_{H_E}) \quad \text{and} \quad \Delta H_r \phi_{E2} = Q_{rx} \left(\frac{S_2}{S} \right) (X_H - X_{H_E}) \quad (5)$$

where X_{H_E} and X_H represent the conversions at heights H_E and H , respectively. Simple first order kinetics and an Arrhenius equation are assumed in the analysis.

5. PREDICTIONS FROM FOUR-ZONE BED-SIDE MODEL

With the model parameters specified in Table 1, the model was solved iteratively. The results are summarized in Table 2. It is seen that for a fast reaction, although 71% conversion is reached in the bottom un-cooled zone with most heat released there, the axial temperature difference is only $\sim 1.5^\circ\text{C}$ due to the vigorous internal solids circulation in the fluidized bed reactor. Similarly, due to the convective particle heat exchange, non-uniform heat removal from heat exchange tubes in the current configuration creates a temperature gradient of only about 3.2°C between the well-cooled zone (B1) and the less-efficiently cooled zone (B2) where steam is being superheated in the corresponding heat exchange tubes. These results suggest that there is little bulk temperature difference between the un-cooled entrance zone and cooled bed zone, as well as between the superheated steam producing (SP) and non-complete boiling (NB) regions in a fluidized bed reactor operated at relatively high gas velocities (0.4 m/s in the current analysis) for group A particles.

6. CONCLUSIONS

Heat transfer from cooling coils immersed in a fluidized bed reactor can be divided into a number of zones in series, corresponding to heating of sub-cooled liquid to the boiling point, boiling itself, and superheating of steam inside the tubes, with some tubes unable to provide complete boiling and therefore showing no superheating zone. A bed-side model was then used to estimate differences in temperature inside the fluidized bed reactor for four zones, corresponding to the regions where steam is being superheated and those where partial boiling is occurring, as well as the un-cooled regions below each of these tube regions. It is shown that, despite differences in heat transfer for the superheating and partially-boiling tubes and the presence of a zone at the bottom where there is no

direct cooling, the differences in temperature are no more than about 1 to 3°C.

NOTATION

A	surface area of cooling tubes, m^2	L_j	jet penetration length, m
C_{pg}	gas thermal capacity, J/kgK	m_{NB}	water flow rate to NB tubes, Kg/s
C_{pp}	particle thermal capacity, J/kgK	m_{SP}	water flow rate to SP tubes, kg/s
D	reactor diameter, m	Q_{rx}	total reaction heat, W
ΔH_r	total reaction heat, W	S	cross-sectional area of reactor, m^2
d_p	particle diameter, mm	T_i	temperature in region i , K
f	fraction of NB stream converted to steam, -	T_w	temperature of cooling tube surface, K
f_d	solid fraction carried up by drift produced by bubble motion, -	T_0	inlet gas temperature, K
f_w	wake fraction of bubbles, -	U	superficial gas velocity, m/s
G_B	total bubble gas flow rate, m^3/s	U_{mf}	minimum fluidization velocity, m/s
h	heat transfer coefficient, W/m^2K	W_a	axial solid mixing rate, kg/s
H	expanded bed height, m	W_r	radial solid mixing rate, kg/s
H_E	height of bottom un-cooled region, m	X_H	conversion at height H , -
k	perimeter parameter in equation (9)	X_{H_E}	conversion at height H_E , -
K_j	interphase mass transfer rate between jet and dense phase, m/s	ε_{mf}	voidage fraction at velocity U_{mf} , -
L	length of cooling tube, m	ϕ_i	conversion in region i , -
		η	correction coefficient for equation(1), -
		ρ_g	gas mixture density, kg/m^3
		ρ_p	particle density, kg/m^3

REFERENCES

1. Botterill, J.S.M., Fluid-Bed Heat Transfer, Academic Press, London, 1975.
2. Molerus, O. and Wirth, K.E., Heat Transfer in Fluidized Beds, Chapman & Hall, London, 1997.
3. Chen, J.C., Heat transfer, Chapter 10 in Handbook of Fluidization and Fluid-Particle Systems, ed. W.C. Yang, Marcel Dekker, New York, 2003, pp.257-286.
4. George, S.E. and Grace, J.R., AIChE Journal, 28, 759-765, 1982.
5. Baeyens, J. and D. Geldart, "Solids mixing," Chapter 4 in Gas Fluidization Technology, D. Geldart ed., J. Wiley & Sons, pp.97-112, 1986.
6. Cliff, R. and J.R. Grace, "Continuous bubbling and slugging," Chapter 3 in Fluidization, J.F. Davidson, R. Cliff and D. Harrison eds., Academic Press, London, pp.73-132, 1985.
7. Grace, J.R. "Fluidized-bed hydrodynamics," Chapter 8.1 of Handbook of Multiphase Systems, ed. G. Hetsroni, Hemisphere, Washington, 1982.
8. Grace, J.R., Generalized Models for Isothermal Fluidized Bed Reactors, in Recent Advances in the Engineering Analysis of Chemically Reacting Systems,

(Ed. L.K. Doraiswamy), Wiley, New Delhi, pp. 237-255 (1984).

9. Merry, J.M.D., Penetration of vertical jets into fluidized beds, *AIChE J.*, 21, 507-510, 1975.
10. Rowe, P.N. and B.A. Partridge, "An X-ray study of bubbles in fluidized beds," *Trans. Instn. Chem. Engrs*, **43**, 157-171, 1965.

Table 1. Parameters used in the current analysis.

	Value	Units	Meaning
A_1	= 26.38	[m ²]	surface area of water/boiling tubes
A_2	= 9.35	[m ²]	surface area of superheated steam tubes
C_{pg}	= 1300	[J/kgK]	gas thermal capacity
C_{pp}	= 756	[J/kgK]	particle thermal capacity
D	= 3.0	[m]	reactor diameter
d_p	= 0.06	[mm]	average particle diameter
h_1	= 182.2	[W/m ² K]	heat transfer coefficient 1
h_2	= 22.3	[W/m ² K]	heat transfer coefficient 2
S_1	= 5.22	[m ²]	cross-sectional area 1
S_2	= 1.85	[m ²]	cross-sectional area 2
T_B	= 400	[°C]	reactor bed temperature
T_0	= 280	[°C]	inlet gas mixture temperature
T_{w1}	= 235	[°C]	surface temperature of cooling tube in boiling region
T_{w2}	= 296	[°C]	surface temperature of cooling tube in superheating region
U	= 0.4	[m/s]	gas velocity
ρ_g	= 0.894	[kg/m ³]	inlet gas mixture density
ρ_p	= 1100	[kg/m ³]	particle density
ΔH_r	= 1,257,000	[W]	total heat released from complete reaction

Table 2. Predicted bed temperature in each zone and conversions.

T_{B1}	398.7 °C	Zone B1
T_{B2}	401.9 °C	Zone B2
T_{E1}	399.9 °C	Zone E1
T_{E2}	402.5 °C	Zone E2
X_{HE}	0.716	Conversion at H_E (zone E)
X_H	0.955	Conversion at H (zone B)

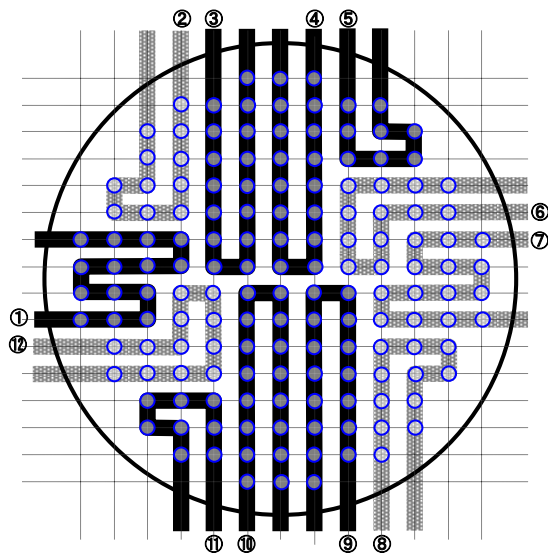


Fig. 1: Plan view of superheated steam-producing tubes (gray) and non-complete boiling tubes (black).

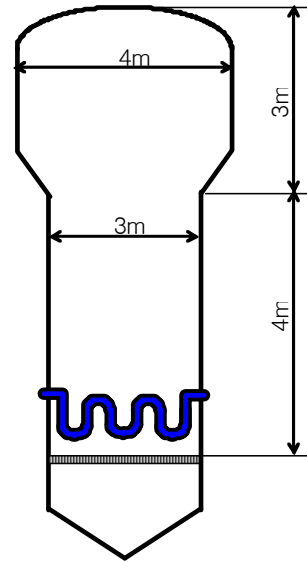


Fig. 2: Schematic of cooling coils in fluidized bed reactor.

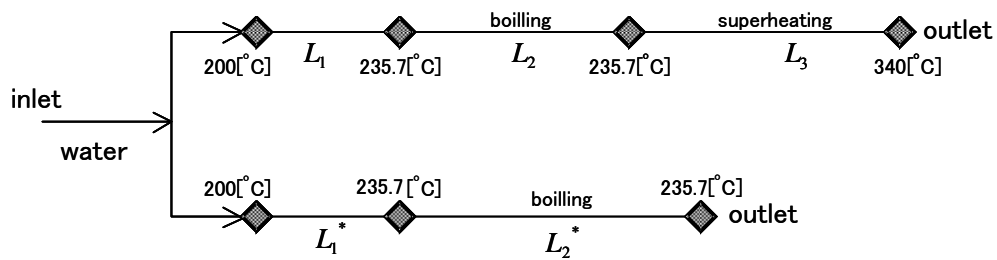


Fig. 3: Schematic showing different sections of total tube length in the blocks where superheating of steam does and does not occur.

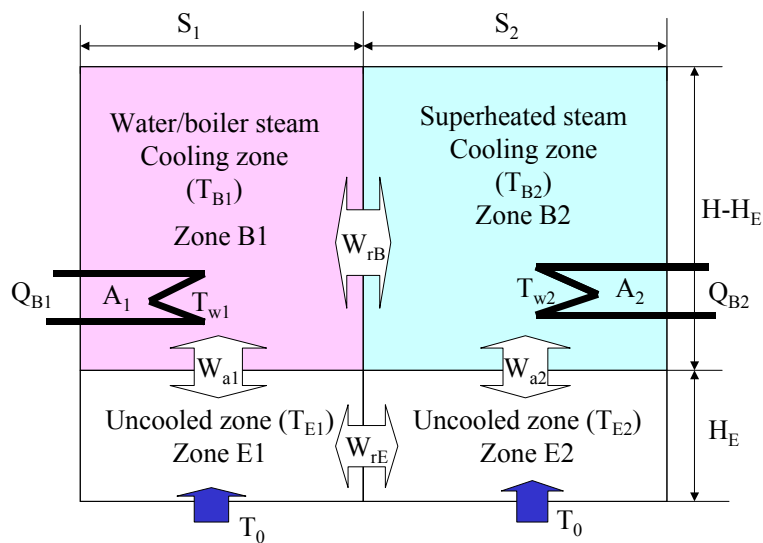


Fig. 4: Four-zone heat exchange model for tube-cooled fluidized bed reactor.

KEYWORDS

Heat transfer, cooling tubes, temperature uniformity, exothermic reactions